On the Importance of 5d Orbitals for Covalent Bonding in Ytterbium Clusters

Yixuan Wang,[†] Friedemann Schautz, Heinz-Jürgen Flad,* and Michael Dolg

Max-Planck-Institut für Physik komplexer Systeme, Nöthnitzer Strasse 38, D-01187 Dresden, Germany

Received: February 11, 1999; In Final Form: April 27, 1999

Ytterbium clusters with three to seven atoms have been studied by means of high-level quantum chemical ab initio calculations using energy-consistent relativistic large- and medium-core pseudopotentials, core-polarization potentials, a coupled-cluster electron correlation treatment, and large valence basis sets up to g functions. We have determined equilibrium structures, cohesive energies, vertical ionization potentials, and electron affinities, as well as vibrational frequencies for clusters with up to six atoms. To demonstrate graphically the transition from van der Waals to covalent interactions with increasing cluster size, the electron localization function (ELF) has been calculated from the Hartree−Fock wave functions for the equilibrium structures obtained from the correlated calculations. Yb clusters behave rather differently from those of group 12, though both have similar equilibrium structures, i.e., they exhibit significantly larger cohesive energies and more pronounced covalent contributions to bonding. We attribute these differences mainly to the presence of low-lying empty d orbitals in Yb, whose role in chemical bonding is qualitatively analyzed.

I. Introduction

The clusters of divalent elements attracted much attention from experimentalists and theoreticians in the past 2 decades (see, e.g., refs 1 and 2 and references therein). A major point of interest is still the size-dependent transition from van der Waals interaction to covalent and finally metallic types of chemical bonding. The most extensively studied element is mercury[1] for which a rather slow transition to the metallic state has been observed. The necessary size of the cluster for which the transition has been accomplished is still controversial, whereby the most recent estimate assumes that it requires at least 400 atoms.[3] Most of the previous theoretical work is based on model Hamiltonians[1] which require some a priori information on the kind of bonding involved. From a theoretical point of view, it seems to be important to study the evolution of properties with the cluster size using methods which do not rely on a specific model. The popular alternative to model Hamiltonians is density functional theory (DFT) which has been applied to group 2 clusters.[4−6] Unfortunately, the presently available functionals do not work well for van der Waals interactions for which the binding energies are either considerably overestimated or no bonding is observed.[7] Especially for small clusters it is therefore desirable to use quantum chemical methods which provide an accurate description of the different kinds of bonding involved. In a recent publication[8] we have studied the onset of the transition from van der Waals to covalent type of bonding for small group 12 clusters using ab initio quantum chemical methods. Although we found clear indications for covalent contributions already for small clusters with $n \leq 6$ atoms, the overall picture shows a dominance of van der Waals interaction for clusters with $n \leq 13$ atoms in agreement with experimental evidence.[9]

Formally, the situation for ytterbium clusters should be analogous to the one of the group 12 elements, since all of them have a valence ns^2 closed-shell electronic configuration. However, Hg ($5d^{10}6s^2$) and Yb ($5d^06s^2$) differ by their 5d shell occupation. This leads to low-energy excited Yb states of 6s → 5d type which are not possible for group 12 metals, where *n*s → *n*p (n = 4, 5, and 6 for Zn, Cd, and Hg, respectively) excitations are lowest, e.g., for Yb the spin−orbit averaged experimental term energy of the ^{3}D (24942 cm^{-1}) state is higher than that of the ^{3}P (18869 cm^{-1}) state, but it is already lower than that of the ^{1}P (25068 cm^{-1}) state.[10] The empty Yb 5d orbitals may also actively, i.e., in the MO-LCAO (molecular orbitals by linear combination of atomic orbitals) sense, take part in chemical bonding, whereas the completely filled Hg 5d shell merely provides a large and easily polarizable core. As a consequence the bonding in Yb clusters will be more complex than for Hg or other group 12 clusters. It has to be investigated to what extent s−d (and possibly p−d) hybridization effects are important for Yb besides the s−p hybridization occurring also for the group 12 metals. With respect to the tendency to form chemical bonds it is known that Hg is rather inert, partly due to relativistic effects ("gold-maximum of relativistic effects",[11] strong stabilization of 6s) but also due to shell structure effects (incomplete shielding of the nuclear charge acting on 6s by the filled 5d and 4f shells[12,13]). Since such effects are either weaker or partly absent for Yb, one may also expect a priori a stronger bonding in Yb clusters than that in Hg clusters.

Alkaline-earth metals also have a valence ns^2 electronic configuration, and for Ca, Sr and Ba an empty $(n-1)$d shell. However, due to the smaller effective nuclear charge on the empty $(n-1)$d shell, it is more diffuse than that for Yb, and states with occupied $(n-1)$d orbitals are less easily accessible. Nevertheless, recent DFT studies by Qureshi and Kumar[14] of Sr clusters indicate that the empty 4d orbitals contribute significantly to the bonding energies as the cluster size grows, expedite the onset of metallicity, and even induce different cluster growth patterns. Thus, for the investigation of Yb clusters it should be even more interesting to understand not only the

* Corresponding author. E-mail: flad@mpipks-dresden.mpg.de. FAX: ++49-(0)-351-871-2199.

[†] Permanent address: Institut of Theoretical Chemistry, Shandong University, 250100 Jinan, People's Republic of China.

10.1021/jp9905169 CCC: $18.00
Published on Web 06/16/1999

size-dependent change of interatomic interactions but also the role the 5d orbitals play for the cluster structures and stabilities.

Only little is known about the properties of Yb clusters from experiment. Suzer and Andrews[15] have observed absorption spectra due to Yb_2 and aggregates larger than the dimer. Rayane et al.[16] and Bréchignac et al.[17] generated Yb clusters using slightly different experimental setups whereby considerably different abundances have been observed, depending critically on the nucleation conditions.

As a starting point for the present theoretical investigation of Yb clusters, three different core definitions for relativistic energy-consistent ab initio pseudopotentials (PP) have been considered, i.e., 42-, 10-, and 2-valence electron PPs have been adjusted (denoted as PP(42), PP(10), and PP(2) in the following).[18] Core-polarization potentials (CPP)[19,20] accounting for both static and dynamic polarization of the PP core are added to PP(10) and PP(2). A careful atomic calibration study of the PPs and a discussion of the calculated spectroscopic properties of the Yb_2 dimer indicate that the medium-core PP(10) and a corresponding CPP yields the most reliable results. The quality of the large-core PP(2) + CPP results also appeared to be quite acceptable, especially in view of the low computational demands of this approach. The potentially most accurate small-core PP(42) calculations turned out to be quite time consuming and an extension to clusters larger than two or three atoms is currently infeasible. The reason is the need to correlate explicitly also several inner shells (e.g., at least 4f, 5s, and 5p) in order to accurately describe the core−valence correlation effects on the weak interatomic interactions. This most costly part of the calculation can be avoided by using a larger core for the PP together with a CPP.

To our knowledge, no other theoretical studies on Yb clusters have been reported in the literature. In the present work we used similar methods as previously for group 12 clusters.[8] The computational results and the analysis of bonding in Yb clusters are compared to our previous findings for the group 12 clusters in order to shed some light on the effect of s−d hybridization on the structure and bonding.

II. Applied Methods and Computational Details

A. Pseudopotentials and Basis Sets. In the calculations reported in this paper we have used energy-consistent scalar−relativistic PPs, i.e., medium-core PP(10) and large-core PP(2), together with the corresponding CPPs.[18] A core−core repulsion correction has been added to PP(2) in order to account for deviations from the point-charge repulsion model between the large Yb^{2+} cores due to the mutual penetration of the electron densities and the concomitant Pauli repulsion. For PP(2), similar valence basis sets as previously used for Hg clusters[21] were applied, i.e., an uncontracted (6s6p5d3flg) basis set for Yb_3 and Yb_4 as well as an uncontracted (6s6p3d2flg) basis set for Yb_5 and Yb_6.

In order to be able to study larger Yb clusters with PP(10), the (9s9p8d6f2g) valence basis set previously used for Yb_2 had to be reduced considerably. After removing the diffuse (2s2p2d) basis functions and reducing the polarization functions to (3flg), a (7s7p6d3flg) basis set results, which was used for Yb_3 and Yb_4. In calibration calculations for Yb_2 this reduced basis set only led to slight deviations in comparison with the better (9s9p8d6f2g) basis set, as can be seen in Table 1. For the study of larger clusters it was necessary to reduce the basis set even further, e.g., (7s7p3d2flg) for Yb_5 and Yb_6, respectively (7s7p3d2f), for Yb_7. Application of these basis sets to Yb_2 shows that (7s7p3d2flg) yields slightly longer bond lengths as well as smaller cohesive energies compared to the best basis set. The loss in accuracy due to the omission of g functions is almost negligible. The consequences of this reduction of the valence basis sets for several quantities of interest are summarized in more detail in Table 1. The basis set superposition error (BSSE) for the PP(10) is rather small; we calculated the counterpoise correction for Yb_2 and found an increase of the bond length of 0.03 Å and a decrease in the binding energy of 0.006 eV, as well as a decrease of the vibrational frequency of 0.4 cm^{-1}. For the larger clusters the BSSE has not been considered.

TABLE 1: Basis Set Dependence of the Bond Length R_e (angstroms), Vertical Ionization Potential IP, and Electron Affinity EA (eV), Cohesive Energy per Atom CE (eV), and Harmonic Vibrational Frequency ω_e (cm^{-1}) for Yb_2 Using PP(10) + CPP and Various Polarization Basis Sets[a]

	8d6f2g		6d3flg		3d2flg		3d2f	
R_e	4.76	4.85	4.78	4.86	4.89	4.96	4.90	4.96
IP	5.50	5.39	5.54	5.39	5.55	5.44	5.56	5.44
CE	0.034	0.032	0.031	0.028	0.026	0.024	0.025	0.024
ω_e	19.6	19.0	19.0	18.4	17.4	16.8	17.4	16.9

[a] The calculations have been done with (first column) and without (second column) correlation of the 5s and 5p shells. Counterpoise corrections for the BSSE are not taken into account.

B. Correlation Treatment. In general both relativistic and electron correlation effects should be simultaneously taken into account in order to obtain reliable results for systems containing heavy elements. For systems with several heavy atoms and a large number of electrons, compromises with respect to computational feasibility and accuracy have to be made. The singles and doubles coupled-cluster method including a perturbative treatment of triple excitations (CCSD(T)) together with the energy-consistent relativistic PP + CCP approach is quite appealing for quantum chemical studies of such systems.[8,21]

Among the standard ab initio methods, the CCSD(T) method is, for cases dominated by a single Hartree−Fock (HF) reference configuration, the one which permits the most accurate treatment of electron correlation. Beyond that it is strictly size extensive, which is of fundamental importance for size-dependence studies in cluster science. We note that a less costly correlation treatment using fourth-order Møller−Plesset perturbation theory was found to significantly overestimate the strengths of van der Waals interactions[22−24] and is not suitable to obtain accurate data. All scalar−relativistic HF and CCSD(T) calculations reported here were performed with the MOLPRO program package.[25]

C. Electron Localization Function. The electron localization function (ELF) was developed by Becke and Edgecombe[26] as a measure for the probability of finding an electron in the neighborhood of another electron with the same spin. By definition, the ELF adopts values between 0 and 1. The higher the ELF value, the smaller is the probability of finding a second electron with the same spin near the reference point. Hence, a large value of ELF means that the reference electron is highly localized. High ELF values locate the regions which can be interpreted as covalent bonds, lone pairs, and inert cores. Low ELF values are typical for the regions between electronic shells and the regions where van der Waals type of interactions dominate. Extensive applications of ELF to various molecules, clusters as well as solids,[8,27] indicate that it yields meaningful, easily understandable, and visually directive patterns of the interactions between vicinal atoms. For the evaluation of ELF and its visualization, separate programs were interfaced to MOLPRO.

The ELF is based on the Hartree−Fock wave function and does not take into account electron correlation explicitly. At first sight this seems to be a major drawback in the present

application with regard to the importance of electron correlation for the bonding in these clusters mentioned above. We argue, however, that most of the qualitative features of covalent interactions are accounted for at the HF level and therefore appear in ELF, provided that structures optimized at the CCSD(T) level are used. Covalent bonding can be also expressed in terms of charge fluctuations[28] which of course strongly depend on the participation of 5d and 6p atomic orbitals to the bonding. In previous papers we compared the degrees of covalency resulting from ELF and correlated respectively uncorrelated charge fluctuations for group 12 dimers.[8,29] For these systems correlation has a major influence on the equilibrium bond length due to van der Waals type dispersion interactions which however do not contribute to the charge fluctuations. Actually, the charge fluctuations were found to be insensitive with respect to electron correlation.[29] The resulting covalent contributions are in qualitative agreement with ELF over a large range of internuclear distances. Therefore it seems to be justified for the evaluation of ELF to take electron correlation only indirectly into account via the optimized structures.

In general, the ELF values in the interaction region are higher for valence-only calculations, i.e., the PP method, than those for all-electron calculations unless the underlying shells are well separated from the valence shell.[30] The same statement certainly holds for PP calculations with different choices of the core and the ELF values from calculations with different PPs are therefore not comparable. In order to arrive at least approximately at the same picture and to be able to compare ELF pictures from different types of PPs, it is necessary to add core orbitals to the valence orbitals obtained with the large-core PP and then compare the resulting ELF to the one of a small-core PP. In a first approximation the small orthogonalization corrections, which would mainly affect the valence shells in the chemically uninteresting core region, can be omitted.

Care has to be taken in order to select the characteristic two-dimensional sections, especially when directional bonding occurs. Characteristic maxima (or minima) of ELF in polyatomic systems may not always be located on straight lines interconnecting two atoms or in planes defined by three atoms. Another aspect to pay attention to is that any interpretation of chemical bonding using ELF should be done in regions inside the van der Waals contour line, i.e., ELF has no physical meaning in regions of very low electron density. In order to facilitate this, we also provide some contour lines of the electron density in our plots, where the outermost contour line of 0.001 au roughly corresponds to the van der Waals "size" of the cluster.

III. Results and Discussion

A. Structures and Cohesive Energies. Even for a small number of closed-shell atoms such as Yb a large variety of more or less likely structures may be proposed. The ultimate approach to this problem would be an unconstrained optimization procedure like the simulated annealing method or molecular mechanics based on an appropriate ab initio method for the electronic energy evaluation. Calculations for the dimer[18] clearly reveals the necessity for an accurate treatment of electron correlation using high-quality correlation methods like CCSD(T) and large basis sets. This renders such optimization procedures impracticable due to the large computational expenses of these methods. As a compromise one can either choose a less accurate but reasonably fast method for the energy evaluation or one can constrain the optimization. Most of the work reported in the literature on the related group 2 elements follow the first course using DFT[4,6,5,14] or effective many-body potentials[31] adjusted to solid state properties. We refrain from this approach since we are mainly interested in the transition from van der Waals to covalent bonding. Present-day DFT does not provide functionals which are appropriate for van der Waals type of interactions. Especially for small clusters this is a severe shortcoming. Model potentials derived from solid state properties are adjusted to metallic type of bonding which is also not appropriate for small clusters. Restricting the optimization procedure seems to be less problematic at least for small clusters. On the basis of the assumption of predominantly van der Waals type of bonding in small Yb clusters, such structures seem to be especially favorable which allow a dense packing of the atoms and maximize the number of nearest neighbor interactions. Therefore, we have considered regular, compact structures in our calculations which fulfill these requirements. The selected structures include equilateral triangular ($n = 3$), tetrahedral ($n = 4$), trigonal bipyramidal and quadrilateral pyramidal ($n = 5$), and octahedral and bicapped tetrahedral ($n = 6$), as well as pentagonal bipyramidal ($n = 7$) structures. The structures have been optimized within the given symmetry using the CCSD(T) method and basis sets discussed above. In order to check whether or not these structures are real local minima, a normal coordinate analysis has been performed for some of these clusters.

TABLE 2: Bond Lengths R_e (angstroms), Vertical Ionization Potentials IP, and Electron Affinities EA (eV), Cohesive Energies per Atom CE (eV), and Harmonic Vibrational Frequencies ω_e (cm^{-1}) for Yb_n ($n = 3-6$) from CCSD(T) Calculations Using the PP(2) + CPP Pseudopotential

	Yb_3	Yb_4	Yb_5	Yb_6[b]
R_e	3.85	3.66	3.59, 3.66[a]	3.50 (3.60, 3.68)
IP	5.17	5.13	4.42	4.11 (4.28)
EA	0.76	0.91	0.81	1.17 (0.96)
CE	0.197	0.457	0.524	0.479 (0.572)
ω_e	51.9 (A'_1)	73.6 (A_1)	82.4, 45.0 (A'_1)	82.7 (A_{1g})
	50.4 (E′)	52.5 (E)	69.9, 41.0 (E′)	47.0 (E_g)
		64.3 (T_2)	66.3 (A''_2)	59.3 (T_{2g})
			55.1 (E″)	62.7 (T_{1u})
				64.8 (T_{2u})

[a] Bond lengths refer to equatorial and axial bonds, respectively. [b] The numbers in parentheses belong to the bicapped tetrahedral structure with bond lengths refering to an edge of the tetrahedron and the distance between a capped and a tetrahedral atom, respectively.

TABLE 3: Same as in Table 2 for Yb_3 and Yb_4 Using the PP(10) + CPP Pseudopotential. For Comparison, Results Are Listed with and without Correlating the 5s and 5p Shells

	5s and 5p shell correlated		5s and 5p shell not correlated	
	Yb_3	Yb_4	Yb_3	Yb_4
R_e	4.30	4.01	4.39	4.10
IP	5.31	5.25	5.20	5.14
EA	0.31	0.56	0.34	0.58
CE	0.096	0.226	0.090	0.206
ω_e	32.4 (A'_1)	52.1 (A_1)	31.0 (A'_1)	49.5 (A_1)
	32.8 (E′)	37.6 (E)	31.3 (E′)	38.4 (E)
		43.8 (T_2)		45.4 (T_2)

Our results obtained by using PP(2) and PP(10) with the corresponding CPPs are summarized in Tables 2−4. The calculated properties include bond lengths (R_e), cohesive energies per atom (CE), vertical ionization potentials (IP), and electron affinities (EA), as well as harmonic vibrational frequencies ω. In our previous work on Yb_2,[18] the large-core PP(2) in connection with a CPP yielded a too short bond length (4.445 vs 4.789 Å) and an excessive CE (0.046 vs 0.031 eV), as well as a too high vibrational frequency (25 vs 19 cm^{-1}), respectively, compared with the corresponding results from the presumably more accurate medium-core PP(10). These quantitative differences in the bonding parameters seem to extend to larger clusters

TABLE 4: Same as in Table 2 for Selected Structures of Yb_5, Yb_6, and Yb_7 Using the PP(10) + CPP Pseudopotential[a]

	Yb_5		Yb_6		
	D_{3h}	C_{4v}	O_h	C_{2v}	Yb_7 (D_{5h})
R_e	4.03, 4.30[b]	4.36, 4.26[b]	4.47	4.12, 4.37[c]	4.52, 4.29[b]
IP	4.65	4.43	4.51	4.55	4.67
EA	0.598	0.85	1.03	0.67	0.69
CE	0.210	0.139	0.166	0.23	0.31
ω_e	50.1, 34.1 (A'_1)		33.1 (A_{1g})		
	45.9, 24.7 (E')		22.5 (E_g)		
	33.8 (A''_2)		16.7 (T_{2g})		
	34.3 (E'')		21.5 (T_{1u})		
			34.0 (T_{2u})		

[a] The results refer to trigonal bipyramidal (D_{3h}) and quadrilateral pyramidal (C_{4v}) structures for Yb_5, octahedral (O_h) and bicapped tetrahedral (C_{2v}) structures for Yb_6, and a pentagonal bipyramidal (D_{5h}) structure for Yb_7. The calculations have been performed without correlating the 5s and 5p shells. [b] The bond lengths respectively refer to equatorial and axial bonds. [c] Respectively, the bond length of an edge of the tetrahedron, the distance between a capped and a tetrahedral atom.

and become even more significant. For example, PP(2) overestimates the cohesive energies per atom of Yb_3 and Yb_4 roughly by a factor of 2 (0.197 and 0.457 eV compared to 0.096 and 0.226 eV, respectively). Even worse, PP(2) reverses the order of orbitals in the case of the octahedral structure of Yb_6. The ground state configuration $1a_{1g}^2f_{1u}^6e_g^4$ obtained with PP(10) becomes $1a_{1g}^2f_{1u}^62a_{1g}^2e_g^2$, yielding a triplet ground state in this case. The results for the triplet state for the octahedral structure and the singlet one for the bicapped tetrahedral structure are listed in Table 2. Significant contributions from d and p basis functions were found for the $2a_{1g}$ orbital by a Mulliken population analysis. We suggest that, despite our hopes mentioned previously,[18] the PP(2) + CPP of Yb is not too suitable for accurate cluster studies due to its failure to simultaneously reproduce core−valence correlation effects for orbitals of different main quantum number (5d, 5f, 6s, and 6p) as well as due to the errors in valence correlation energies arising from the use of nodeless pseudovalence orbitals of different main quantum numbers (5d and 6s,6p).

We now turn to the results from the PP(10) + CPP calculations. For Yb_3 and Yb_4, the calculations were carried out both with and without correlation of the 5s and 5p semicore shells using identical basis sets. It was found that the inclusion of 5s and 5p in the active orbital space only results in a small bond length contraction (roughly 0.09 Å for each cluster) and an insignificant increase of the cohesive energy per atom (0.006 eV for Yb_3, 0.02 eV for Yb_4). The relative differences in the other properties, i.e., IP, EA, and the vibrational frequencies, remains about 5%. This can be understood in terms of various shell contributions to the atomic static dipole polarizability. Core−valence correlation can be described in a semiclassical manner in terms of the polarizability of the core in the field of the valence electrons, which is exactly the idea used in the construction of the CPP. Test calculations using the small-core PP(42) pseudopotential revealed that only 8% of the correlation contributions to the static dipole polarizability of the $4d^{10}4f^{14}5s^25p^66s^2$ configuration are due to the 5s and 5p shells. Neglecting these shells in the correlation treatment is therefore justified. The dominant contributions to core−valence correlation which are due to the 4d and 4f shells are included through the CPP in our approach.

In order to be able to go beyond Yb_4, only electrons in the sixth shell are explicitly correlated at the CCSD(T) level using PP(10) with CPP. As mentioned above also reduced basis sets had to be applied. The calculated trigonal (D_{3h}) bipyramid and

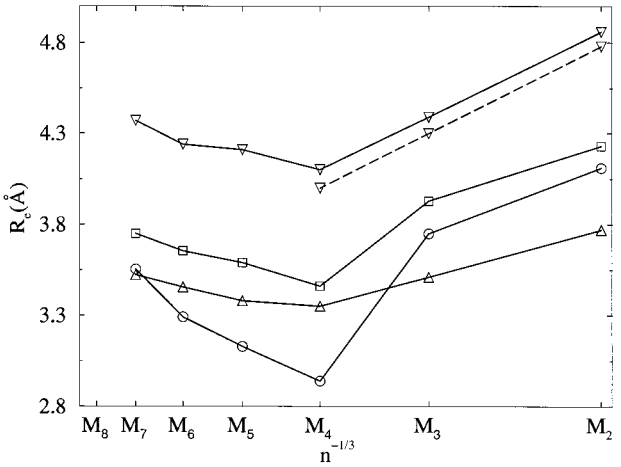

Figure 1. Averaged bond lengths $\bar{R}_e$ (angstroms) for the nearest-neighbor interaction in Yb ▽, Zn ○, Cd □, and Hg △. The solid and dashed lines refer to the results from the PP(10) + CPP calculations without and with fifth shell electrons correlated, respectively.

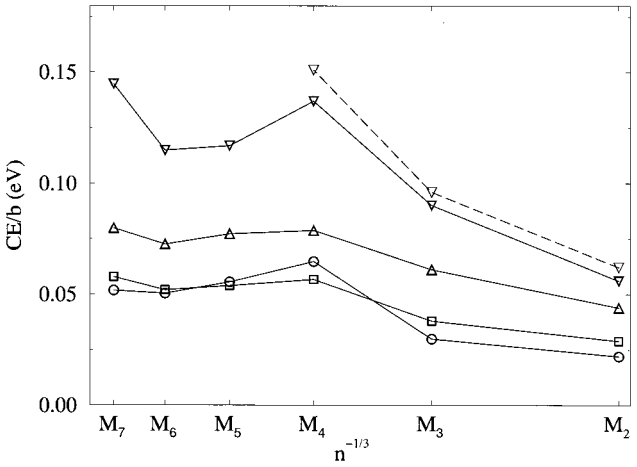

Figure 2. Dissociation energies per nearest-neighbor interaction CE/b (eV). The symbols have the same meanings as in Figure 1.

quadrilateral (C_{4v}) pyramid of Yb_5 have two types of atoms: axial and equatorial, or peak and base, respectively, leading to two types of bonds. The length of the equatorial bond in D_{3h} is very close to that of the Yb_4 tetrahedral structure (4.03 vs 4.10 Å), whereas that of the axial bond is longer by 0.2 Å. The rather large difference between the axial and equatorial bond lengths can be attributed to the different number of nearest-neighbor interactions for the axial and equatorial atoms. In the case of the C_{4v} structure, however, the peak-to-base bond length is shorter than the base bond length by 0.1 Å. It turns out that the D_{3h} structure is lower in energy by 0.36 eV and has a slightly shorter averaged bond length by 0.1 Å than that C_{4v} structure, similarly to previous findings for Hg_5.[21] The bicapped tetrahedral structure for Yb_6 occurs to be more stable than the octahedral one by about 0.38 eV, and its averaged bond length is also shorter by 0.2 Å. The bond lengths in the tetrahedral skeleton agree well with those of Yb_4, i.e., 4.12 vs 4.10 Å. Similar results have been predicted for the homologues of the group 12 atoms. In contrast to the PP(2) + CPP calculations we obtained a singlet ground state for the octahedral structure similar to the group 12 clusters. MRCI calculations for the triplet ^3E_g state with $1a_{1g}^2f_{1u}^6e_g^32a_{1g}^1$ configuration give a rather small singlet−triplet splitting of 0.65 eV. The bond lengths of the ^3E_g state are overall shortened by 0.3 Å showing a Jahn−Teller distortion accompanied by a Jahn−Teller splitting of 0.12 eV.

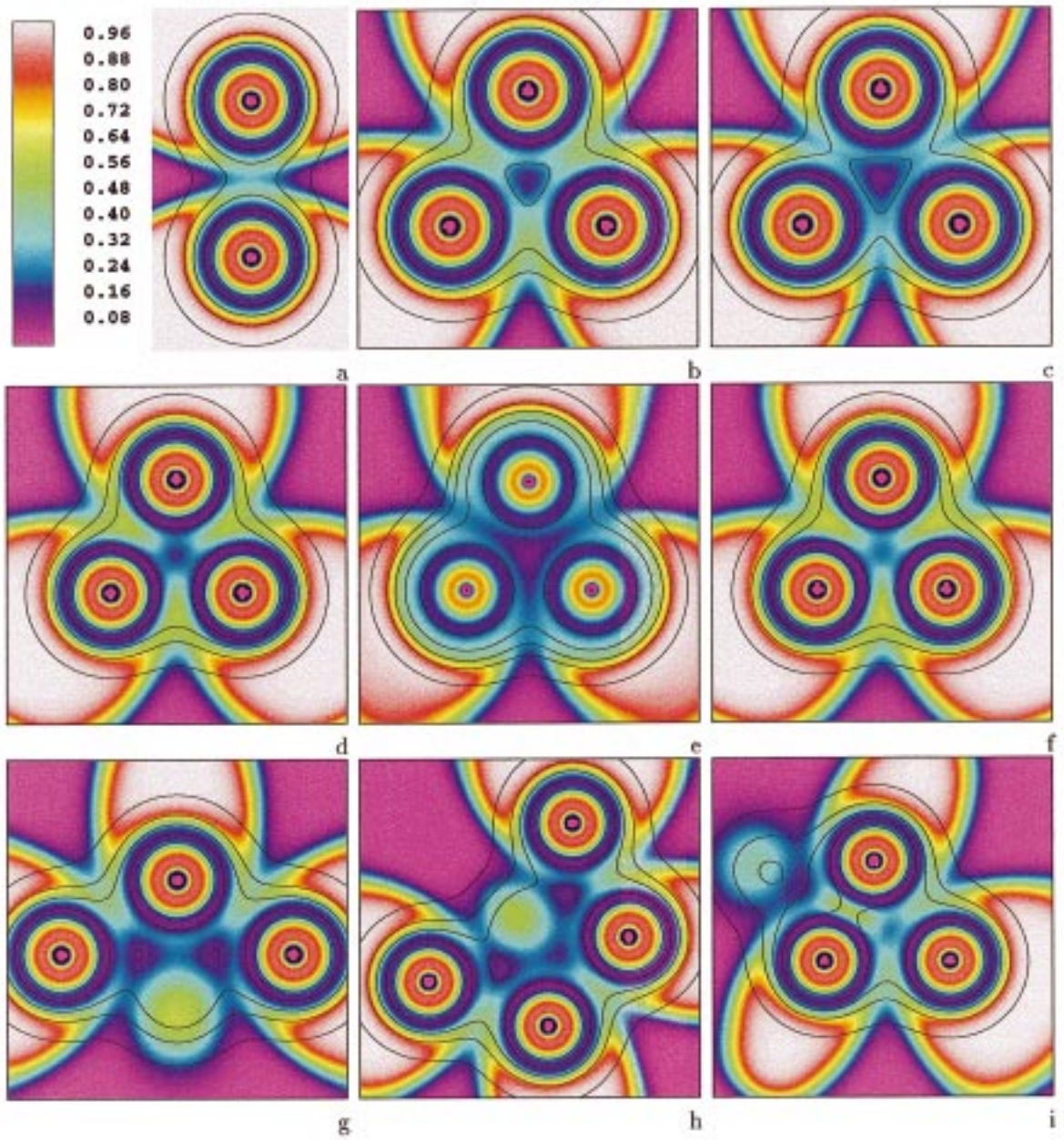

Figure 3. 2D plots of ELF. The ELF values are encoded by colors and overlayed by contour lines of the electron densities. The outmost contour line of 0.001 indicates the approximate "size" of the cluster. The plots refer to PP(10) + CPP calculations unless otherwise noted. Dimer (a) Yb_2; equilateral triangular structure (b,c) Yb_3 with and without d orbitals; surface of the tetrahedral structure (d) Yb_4; (e) Zn_4 (PP(2) + CPP calculation, pseudocore orbitals added); equatorial plane of the trigonal bipyramidal structure (f) Yb_5; section through two axial and one equatorial atom of the trigonal bipyramidal structure (g) Yb_5; section through two capped and two tetrahedral atoms of the bicapped tetrahedral structure (h) Yb_6; section through two axial and one equatorial atom of the pentagonal bipyramidal structure (i) Yb_7.

For the pentagonal bipyramid of Yb_7 with D_{5h} symmetry, the equatorial bond length is larger than the axial bond length by approximately 0.2 Å, while the distance between two axial atoms (3.83 Å) is markedly shorter than the latter one by about 0.5 Å. The two axial atoms are pressed together due to the interactions with the equatorial atoms leading to this exceptionally short bond distance.

The size dependencies of the averaged bond length $\bar{R}_e$ and the dissociation energy per nearest-neighbor interaction (CE/*b*) are shown in Figures 1 and 2, respectively. Only the most stable structures are included for those cases where two structures were calculated. For comparison, we have also shown the corresponding results for the group 12 clusters. The averaged bond length curve exhibits a local minimum for Yb_4 which corresponds to a local maximum in the CE/*b*. This result indicates the exceptional stability of the tetrahedral structure where Yb resembles the group 12 clusters. In general Yb clusters have longer bonds and higher dissociation energies compared to group 12 clusters. This indicates larger covalent bonding contributions in Yb clusters compared to their group 12 homologues.

B. Bonding Analysis Using ELF. One of the major advantages of ELF is that it can directly reveal the character of bonding between two atoms, i.e., one can easily distinguish between van der Waals and covalent interactions. Generally, a low-valued saddle point exists in the ELF values between two atoms for a pure van der Waals interaction, while a high-valued maximum occurs for typical covalent interactions. ELF is especially suitable to investigate the transition between different types of bonding.

Figure 3a shows ELF for Yb_2. One observes a saddle point of ELF = 0.29 between the atoms. Although this ELF value is much higher than the values for the group 12 homonuclear

dimers, (0.05, 0.05, and 0.06 for Zn_2, Cd_2, and Hg_2 respectively) qualitatively the bonding between the atoms is still dominated by van der Waals interactions. A similar conclusion was obtained by a completely independent method, i.e., the analysis of charge fluctuations, by two of the present authors.[18] However, the ELF for Yb_3 exhibits a characteristic difference, a green region of high ELF values between a pair of atoms (ELF = 0.46) (Figure 3b). This clearly indicates that the covalent bonding contributions in Yb_3 are significantly increased compared to the dimer, which is also in accordance with the observed trends for the bond length (Figure 1) and the cohesive energy per nearest-neighbor interaction (Figure 2). It is interesting to analyze which atomic orbitals cause the covalent contribution in Yb_3. If d functions are excluded in the HF calculation, the ELF values in the region between the atoms are considerably reduced (ELF = 0.31) (Figure 3c). The still stronger covalent interactions for Yb_4 are visualized by the green−yellow interatomic region of high ELF values which even exhibits a local maximum (ELF = 0.55) (Figure 3d). It is noticed that the maximum somewhat deviates from the interatomic axis. This behavior is well-known from covalent bound systems with high strain, e.g., carbosilane,[32] where the possible bonding angles of the sp^n hybridization do not agree with those dictated by the number of atoms. As a consequence of this deviation the position of the 3D maximum is not exactly in the plane depicted in Figure 3d. Again, excluding d functions lowers the ELF values between the atoms (ELF = 0.39) significantly. It is important to note that the influence of d functions on the corresponding ELF pictures of the group 12 clusters is negligible. Therefore it seems to be evident that already in small Yb clusters a hybridization between 6s and 5d orbitals occurs which leads to significant covalent contributions to bonding. For the group 12 clusters the 5d shell is fully occupied and cannot contribute to bonding in a similar fashion. For comparison we have shown the same plane for the corresponding Zn_4 cluster (Figure 3e) which exhibits the largest covalent contributions among the small group 12 clusters.

The situation remains quite similar for Yb_5. As it has to be expected the ELF pictures of the triangular bipyramidal and tetrahedral structure are very similar. However, because of symmetry the 3D maximum is exactly located on the plane through the three equatorial atoms (Figure 3f). Because of the different bond lengths for the equatorial and the axial bonds, the covalent contributions to the latter are slightly weaker (Figure 3g).

In the case of the bicapped tetrahedral structure of Yb_6, Figure 3h shows a plane which includes the two capped and two tetrahedral atoms. The covalency within the tetrahedral skeleton (ELF = 0.46) is slightly lower than in the corresponding Yb_4 cluster (ELF = 0.55), although the bond lengths are nearly the same. However, the covalent interactions between the capped and tetrahedral atoms (ELF = 0.44) are only slightly weaker despite the larger bond lengths.

An especially interesting case are the two axial atoms of Yb_7 which possess the shortest bond distance among all of the clusters considered in this work. Figure 3i shows a region of high ELF values squeezed together between the cores of the axial atoms. As already mentioned in the last subsection, the short distance between the two axial atoms of Yb_7 results from the fact that there are five axial interactions for each axial atom.

C. Ionization Potentials and Electron Affinities. Vertical ionization potentials (IP) and electron affinities (EA) have been calculated by the CCSD(T) method with only 6s shell electrons correlated beyond Yb_4 clusters. It can be seen from Table 3 that the effect of this approximation on the IP and EA of Yb_3 respectively Yb_4 is rather small. The size dependency of the IP is presented in Figure 4. For comparison we have also included results for group 12 clusters. The changes of the IP with cluster size for Yb and Hg look very similar. The behavior of the IP provides no indication on the completely different evolution of covalency in the clusters of these elements. Beyond that, the IPs of different structures of the same cluster size are rather similar. This has been observed for the D_{3h} bipyramid and the C_{4v} pyramid for Yb_5 where the difference is only 0.18eV and for the octahedral and bicapped tetrahedral structure for Yb_6 for which the IPs are nearly identical, although bond lengths and CEs are quite different in both cases.

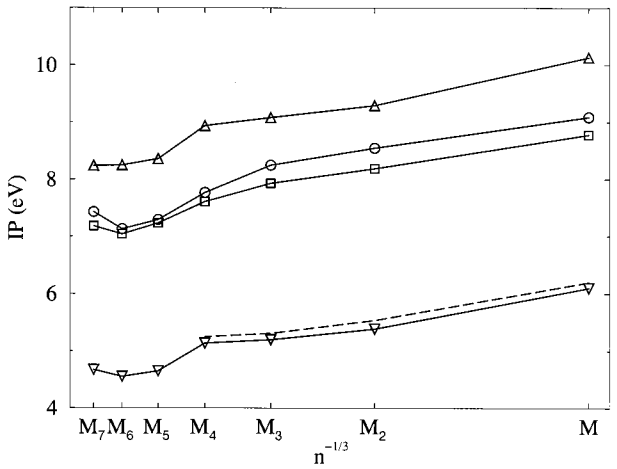

Figure 4. Vertical ionization potentials IP (eV) for Yb and the corresponding group 12 clusters. The symbols have the same meanings as in Figure 1.

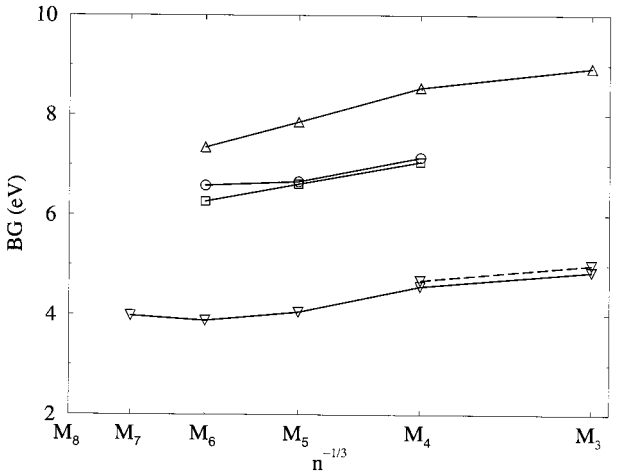

Figure 5. The "band gap" BG = IP − EA (eV) for Yb and the corresponding group 12 clusters. The symbols have the same meanings as in Figure 1.

We also observed that less stable structures have somewhat larger vertical electron affinities. In contrast to the behavior of Hg clusters where the correlation contribution to the IP decreases rapidly and disappears for Hg_4,[21] it decreases slowly from 0.32 eV for Yb_2 to 0.29 eV for Yb_4 and remains approximately constant at a value of 0.20 eV for the other examined clusters.

More interesting than the individual properties IP and EA is their difference BG = IP − EA shown in Figure 5. In solids BG is the band gap and in a one-particle picture it roughly corresponds to the splitting between the highest occupied and the lowest unoccupied orbitals (molecules, clusters) or Bloch functions (polymers, solids). We adopt the definition BG = IP

− EA also for clusters in order to be able to go beyond theone-particle picture, i.e., to include electron correlation effects. For Yb and group 12 clusters one has a predominant van der Waals interaction for the dimers (BG ≫ 0) and a metallic one for the bulk (BG = 0). In between covalent contributions arise and a decrease of BG is observed. Therefore, BG is also a suitable quantitative global measure of covalent contributions to bonding in clusters. As has been shown above in the analysis using ELF that the local bonding characteristics within a cluster may depend on the environment of the atoms under consideration. BG significantly decreases from Yb_3 to Yb_5 by 0.8 eV, and therefore the covalent contributions to bonding considerably increase. Beyond Yb_5 the decrease of BG becomes slower.

D. Vibrational Frequencies. Since we have optimized our structures under certain symmetry constraints, it is important to check whether they are stable against small unconstrained structural distortions. A harmonic vibrational analysis has to be performed in each case which requires the calculation of the second derivatives of the energy expectation value with respect to a set of internal coordinates. As we have mentioned above, Yb clusters depend strongly on electron correlation: the available HF (or MP2) programs for frequency calculations, based on analytic second derivatives, are therefore not suitable for our purpose. Moreover, neither first nor second analytic derivatives have been derived or implemented for the CPP, which is of central importance in the PP Hamiltonian and should not be omitted in frequency calculations. A straightforward numerical differentiation using the CCSD(T) method is too costly from the computational point of view. We have therefore restricted ourselves to highly symmetrical clusters where one can apply group theory to decompose the problem into one and two dimensional independent subproblems. The remaining small number of second derivatives can be calculated numerically using the CCSD(T) method. A detailed exposition of the techniques involved are given in the book of Wilson et al.[33] Further technical details of our calculations are described elsewhere.[8]

Vibrational frequencies have been calculated for the equilateral triangular, tetrahedral, triangular bipyramidal, and octahedral structures; the results are given in Tables 2−4. First of all we want to mention that all frequencies are real, i.e., all of our examined structures represent real local minima and are therefore stable against small structural distortions. In order to compare our results with the group 12 clusters we have shown the averaged vibrational frequencies, calculated as the weighted average of all modes, in Figure 6. The averaged frequencies of the Yb clusters behave qualitatively very similar to those of Cd and Hg, but quite different from those of Zn at least for three and four atoms. The exceptional stability of the tetrahedral structure is also represented by a local maximum in the averaged frequencies.

IV. Conclusions

The electronic properties of small Yb clusters were found to be significantly different from the related group 12 clusters. The evolution of covalent bonding with increasing cluster size occurs much faster for Yb cluster. Clear indications for this can be obtained from ELF pictures and the strong increase of the cohesive energy compared to the corresponding group 12 clusters. This is due to unoccupied atomic 5d orbitals which contribute significantly to the covalent bonding as can be seen from ELF.

We demonstrated the necessity to use the medium-core PP-(10) + CPP pseudopotentials in contrast to group 12 clusters where the large-core PP(2) + CPP pseudopotentials work quite well. The failure of the large-core pseudopotential is probably due to its inconsistent treatment of core-valence correlation for orbitals of different main quantum number (5d versus 6s,6p). Using PP(10) + CPP pseudopotentials increases the computational expense significantly in calculations with correlated 5s,-5p electrons. We found that without essential loss of accuracy one can restrict the correlation treatment to the 6s electrons which makes the overall computational effort comparable to calculations using the PP(2) + CPP pseudopotential.

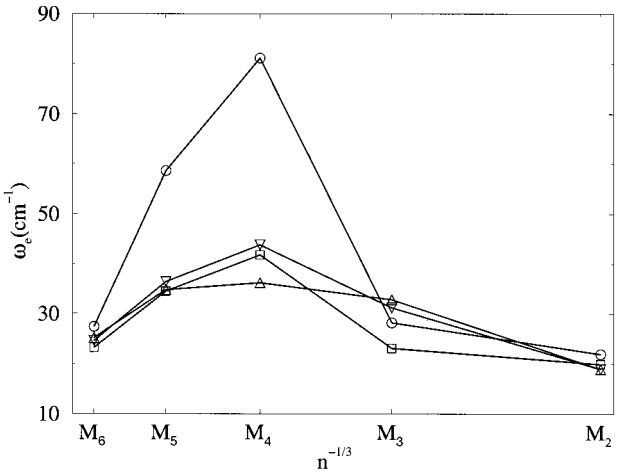

Figure 6. The averaged vibrational frequencies $\bar{\omega}_e$ (cm^{-1}) for Yb and the corresponding group 12 clusters. The symbols have the same meanings as in Figure 1.

Acknowledgment. The authors are grateful to Dr. A. Savin, Paris, for providing us with his ELF program and to Prof. P. Fulde, Dresden, for continuous support.

References and Notes

(1) Pastor, G. M.; Bennemann, K. H. In *Clusters of Atoms and Molecules, Vol. I*; Haberland, H. Ed.; Springer: Berlin, 1994; p 86.
(2) de Heer, W. A. *Rev. Mod. Phys.* **1993**, *65*, 611.
(3) Busani, R.; Folkers, M.; Cheshnovsky, O. *Phys. Rev. Lett.* **1998**, *81*, 3836.
(4) Kawai, R.; Weare, J. H. *Phys. Rev. Lett.* **1990**, *65*, 80.
(5) Kumar, V.; Car, R. *Z. Phys. D.* **1991**, *19*, 177.
(6) Boutou, V.; Allouche, A. R.; Spiegelmann, F.; Chevaleyre, J.; Aubert Frécon, M. *Eur. Phys. J. D* **1998**, *2*, 63.
(7) Pérez-Jordá, J. M.; Becke, A. D. *Chem. Phys. Lett.* **1995**, *233*, 134.
(8) Flad, H.-J.; Schautz, F.; Wang, Y.; Dolg, M.; Savin, A. *Eur. Phys. J. D.* **1999**, *6*, 243.
(9) Haberland, H.; Kornmeier, H.; Langosch, H.; Oschwald, M.; Tanner, G. *J. Chem. Soc., Faraday Trans.* **1990**, *86*, 2473.
(10) Martin, W. C.; Zalubas, R.; Hagan, L. *Atomic Energy Levels−The Rare Earth Elements*; NSRDS-NBS-60; National Bureau of Standards, U.S. Department of Commerce: Washington, DC, 1978.
(11) Pyykkö, P. *Chem. Rev.* **1988**, *88*, 563.
(12) Bagus, P. S.; Lee, Y. S.; Pitzer, K. S. *Chem. Phys. Lett.* **1975**, *33*, 408.
(13) Seth, M.; Dolg, M.; Fulde, P.; Schwerdtfeger, P. *J. Am. Chem. Soc.* **1995**, *117*, 6597.
(14) Qureshi, T.; Kumar, V. *d-Electron induced icosahedral growth in strontium clusters*; condmat/9806167.
(15) Suzer, S.; Andrews, L. *J. Chem. Phys.* **1988**, *89*, 5514.
(16) Rayane, D.; Benamar, A.; Melinon, P.; Tribollet, B.; Broyer, M. *Z. Phys. D* **1991**, *19*, 191.
(17) Bréchignac, C.; Cahuzac, Ph.; Carlier, F.; de Frutos, M.; Masson, A.; Roux, J. Ph. *Z. Phys. D.* **1991**, *19*, 195.
(18) Wang, Y.; Dolg, M. *Theor. Chem. Acc.* **1998**, *100*, 124.
(19) Müller, W.; Flesch, J.; Meyer, W. *J. Chem. Phys.* **1984**, *80*, 3297.
(20) Fuentealba, P.; Preuss, H.; Stoll, H.; von Szentpály, L. *Chem. Phys. Lett.* **1982**, *89*, 418.
(21) Dolg, M.; Flad, H.-J. *Mol. Phys.* **1997**, *91*, 815.

(22) Schwerdtfeger, P.; Li, J.; Pyykkö, P. *Theor. Chim. Acta* **1994**, *87*, 313.

(23) Dolg, M.; Flad, H.-J. *J. Phys. Chem.* **1996**, *100*, 6147.

(24) Yu, M.; Dolg, M. *Chem. Phys. Lett.* **1997**, *273*, 329.

(25) MOLPRO is a package of ab initio programs. Werner, H.-J.; Knowles, P. J.; Almlof, J.; Amos, R. D.; Deegan, M. J. O.; Elbert, S. T.; Hampel, C.; Meyer, W.; Peterson, K.; Pitzer, R. M.; Stone, A. J.; Taylor, P. R.; Werner, H.-J.; Knowles, P. J. *Theor. Chim. Acta* **1990**, *78*, 175. Hampel, C.; Peterson, K.; Werner, H.-J. *Chem. Phys. Lett.* **1992**, *190*, 1.

(26) Becke, A. D.; Edgecombe, K. E. *J. Chem. Phys.* **1990**, *92*, 5397.

(27) Savin, A.; Nesper, R.; Wengert, S.; Fässler, T. F. *Angew. Chem., Int. Ed. Engl.* **1997**, *36*, 1808 and references therein.

(28) Fulde, P. *Electron Correlations in Molecules and Solids*, 2nd ed.; Springer: Berlin, 1993.

(29) Schautz, F.; Flad, H.-J.; Dolg, M. *Theor. Chem. Acc.* **1998**, *99*, 231.

(30) Kohout, M.; Savin, A. *J. Comput. Chem.* **1997**, *12*, 1431.

(31) Hearn, J. E.; Johnston, R. L. *J. Chem. Phys.* **1997**, *107*, 4674.

(32) Savin, A.; Flad, H.-J.; Flad, J.; Preuss, H.; von Schnering, H. G. *Angew. Chem.* **1992**, *104*, 185; *Angew. Chem., Int. Ed. Engl.* **1992**, *31*, 187.

(33) Wilson, E. B., Jr.; Decius, J. C.; Cross, P. C. *Molecular Vibrations*; McGraw-Hill: New York, 1955.